



Characterization of InGaAs quantum dot lasers with a single quantum dot layer as an active region

Richard P. Mirin^{a,b,*}, Arthur C. Gossard^b, John E. Bowers^b

^a Optoelectronic Manufacturing Group, National Institute of Standards and Technology, 325 Broadway, Boulder, CO 80303, USA

^b Department of Electrical and Computer Engineering, University of California, Santa Barbara, Santa Barbara, CA 93106, USA

Abstract

Quantum dot lasers with an active region consisting of just a single quantum dot layer have been grown using molecular beam epitaxy and characterized from 80 to 300 K. The quantum dot lasers lase from excited states over the entire temperature range. The characteristic temperature is 185 ± 10 K over the temperature range 80–141 K and decreases to 111 ± 2 K from 141–304 K. The effects of scattering by the quantum dots has also been analyzed and shown to be unimportant in these quantum dot lasers. © 1998 Elsevier Science B.V. All rights reserved.

Keywords: Quantum dot lasers; Rayleigh scattering

1. Introduction

Quantum dot lasers have been proposed as improved structures as compared to quantum well or bulk lasers [1,2]. Improvements such as insensitivity of threshold current to temperature [1] and decreased threshold current and increased differential gain [2] have been predicted for quantum dot lasers, based on the assumption of a delta function density of states. Until recently, however, fabrication of quantum dot lasers has not been possible due to the difficulty of forming dense arrays of uniform quantum dots with high radiative efficiency.

Quantum dots formed by the Stranski–Krasnow transition of highly strained $\text{In}_x\text{Ga}_{1-x}\text{As}$

grown on GaAs by molecular beam epitaxy (MBE) or organometallic vapor phase epitaxy (OMVPE) have recently been demonstrated by several groups [3–8]. These quantum dots are coherently strained to the GaAs substrate, and they emit bright room-temperature photoluminescence (PL). Despite the broad line widths seen in PL (~ 40 – 50 meV), room temperature operation of quantum dot lasers has been demonstrated by several groups, including both lasers with only one layer of quantum dots [9–11] and lasers with multiple layers of quantum dots [12–14]. The main difference between the use of multiple layers as compared to single layers has been the ability to obtain ground-state lasing at room temperature with the use of multiple layers. Single layer quantum dot lasers do not have enough gain at the ground-state transition energy to lase at that energy. Instead, lasing occurs from

* Corresponding author. Tel.: 303 497 7955; fax: 303 497 3387; e-mail: mirin@boulder.nist.gov.

excited states in these lasers. In this paper, we will discuss the experimental characteristics of some quantum dot lasers that have only a single layer of quantum dots as the active region, as well as discuss a possible loss mechanism due to scattering by the quantum dots.

2. Experimental results

The growth (using molecular beam epitaxy) and processing of the quantum dot lasers has already been described [11,15] and will only be summarized here. Two wafers have been grown with identical epilayer structures except for the active region. A quantum well laser is grown that has an active layer that corresponds to the thickness of the Stranski–Krastanow wetting layer. A quantum dot laser is grown that contains a single layer of quantum dots with an areal density of about $5 \times 10^{10} \text{ cm}^{-2}$. The lasers are processed into $50 \mu\text{m}$ wide stripes with a wet-etched mesa geometry.

Fig. 1 shows output power versus current ($L-I$) curves for $50 \mu\text{m} \times 800 \mu\text{m}$ quantum dot and quantum well lasers taken at 293 K under pulsed operation. Several devices of different lengths have been measured, and the reciprocal of external differential efficiency has been plotted versus length in order to extract the internal differential quantum efficiency, η_d , and the internal loss, α_i . The quantum dot laser has an η_d of 81% and an α_i of 35 cm^{-1} . The quantum well laser has an η_d of 70% and an α_i of 7 cm^{-1} .

Fig. 2 shows $L-I$ curves at various temperatures for the quantum dot laser. The threshold current density decreases as the laser is cooled. Despite this decrease in threshold current density, the quantum dot laser lases from excited states over the entire temperature range. However, the decrease in threshold current density corresponds to a reduction in state filling that compensates the increase in band gap with decreasing temperature. This leads to a laser whose lasing wavelength depends very weakly on temperature [11].

Fig. 3 shows a plot of threshold current density versus temperature for the quantum dot and quantum well lasers. The characteristic temperature, T_0 ($I = I_0 \exp(T/T_0)$), is extracted from this plot.

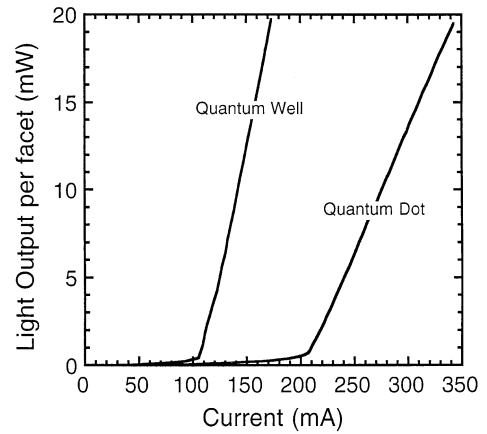


Fig. 1. Pulsed $L-I$ curves taken at room temperature on quantum well and quantum dot lasers with dimensions of $50 \mu\text{m} \times 800 \mu\text{m}$.

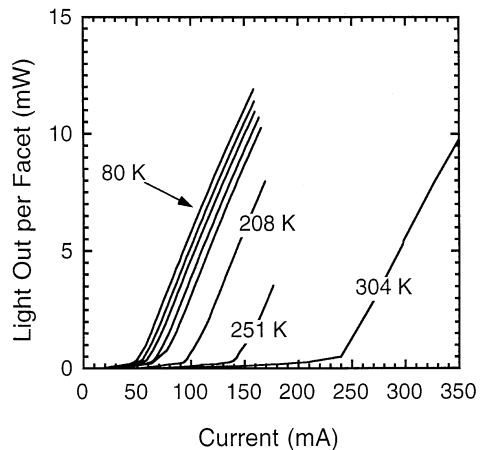


Fig. 2. Temperature-dependent $L-I$ curves measured on a quantum dot laser. Each curve is taken with a temperature increase of 21% from the previous curve.

For the quantum dot laser, T_0 is $185 \pm 10 \text{ K}$ over the temperature range 80–141 K and $111 \pm 2 \text{ K}$ over the range 155–304 K. For the quantum well laser, T_0 is $173 \pm 6 \text{ K}$ over the temperature range 80–171 K and $95 \pm 2 \text{ K}$ from 208–304 K. The small improvement in T_0 seen in the quantum dot lasers as compared to the quantum well lasers is not as dramatic as has been predicted by Arakawa and Sakaki [1]. However, their calculations assume that the lasing occurs from the ground states of the

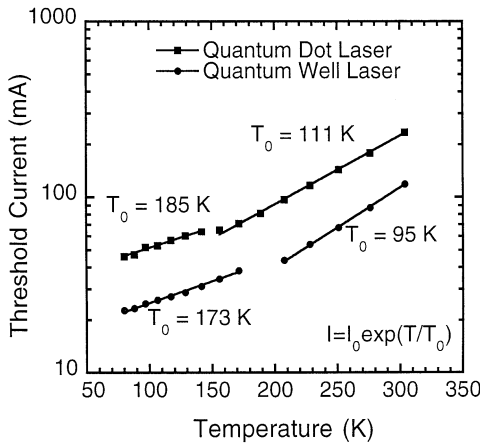


Fig. 3. Threshold current density versus temperature for the quantum well and quantum dot lasers. The characteristic temperature is extracted from a curve fit to the data over some temperature range.

quantum dots and the excited states are negligibly populated. This does not represent the quantum dot lasers studied here, in which lasing occurs from excited states. Therefore, we do not expect to observe extremely high characteristic temperatures in these single layer quantum dot lasers.

3. Scattering by quantum dots

In a typical edge-emitting laser with a quantum well active region, the optical mode sees a constant effective modal refractive index as it propagates along the waveguide. However, in a quantum dot laser the refractive index varies because the layer of quantum dots is not continuous. Any refractive index discontinuity can cause optical scattering and therefore optical loss. Because the quantum dots are much smaller than the wavelength of the light, we must consider Rayleigh scattering as a possible scattering mechanism. Particles are of the proper size to be Rayleigh scatterers if they meet the criterion that the radius of the particle, a , is less than about $\frac{1}{10}$ of the wavelength of light. For the quantum dots that are studied here, the wavelength of light in the semiconductor waveguide is about 325 nm. Thus, in order to be of the proper size for Rayleigh scattering, the quantum dot radius should

be less than about 32 nm. The quantum dots investigated here are pyramid-shaped with a maximum dimension of about 15 nm and thus satisfy the size limits for Rayleigh scatterers. Limitations imposed on quantum dot lasers due to Rayleigh scattering losses will be discussed.

The derivation of single-particle Rayleigh scattering from spherical particles is well-known, and only the important results are summarized here. For a more detailed description of Rayleigh scattering see Ref. [16]. The scattering cross section per particle is given by

$$C_{\text{scat}} = \frac{128\pi^5 a^6}{3\lambda^4} \left(\frac{n^2 - 1}{n^2 + 2} \right)^2, \quad (1)$$

where a is the radius of the Rayleigh scatterer, λ is the wavelength of light in the surrounding medium, and n is the ratio of the refractive indices, n_1/n_2 , where n_2 (n_1) is the refractive index of the surrounding medium (scatterer). Note that scattering strength depends on the size of the particle to the 6th power.

The total scattering loss due to some density of particles per unit volume, ρ_v , is usually given by $C_{\text{scat}}\rho_v$. However, for the special case of a waveguide configuration where the particles are not uniformly dispersed throughout the entire waveguide, some slight modification is needed. Only the fraction of the photons in the waveguide that interact with the quantum dots can be scattered. This fraction is given by the so-called modal confinement factor, Γ , which is given by Ref. [17]

$$\Gamma = \frac{\int_{-w/2}^{w/2} \int_{-d/2}^{d/2} |U(x, y)|^2 dx dy}{\iint_{xy} |U(x, y)|^2 dx dy}, \quad (2)$$

where $U(x, y)$ is the normalized transverse electric field profile and $w(d)$ is the lateral (transverse) dimension of the semiconductor active region. Thus,

$$\alpha_{\text{RS}} = \Gamma C_{\text{scat}}\rho_v, \quad (3)$$

gives the net attenuation due to Rayleigh scattering.

We now examine the limits that Rayleigh scattering imposes on our lasers. For these calculations we will assume that the index of the scatterer, n_1 , is 3.7 (which is approximately the refractive index of bulk InAs at 1000 nm), the index of the surrounding

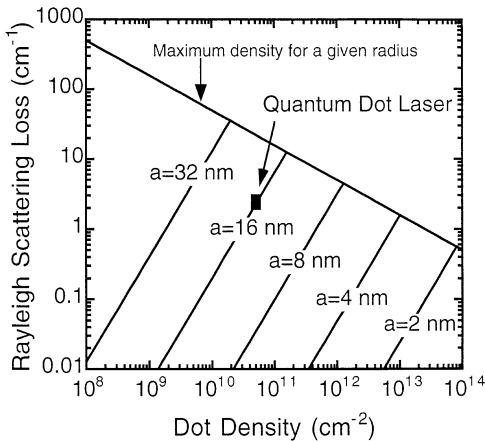


Fig. 4. Rayleigh scattering loss from the quantum dots. Each curve indicates the Rayleigh scattering loss for a given quantum dot radius over a range of areal quantum dot densities. Each curve terminates on the horizontal solid line that represents the maximum packing density of spherical quantum dots for a given radius, i.e., the dots are just in contact with one another.

medium, n_2 , is 3.2 (which is approximately the effective modal refractive index of the wave guide at 1000 nm), and λ is 325 nm. Fig. 4 shows a plot of Rayleigh scattering loss versus areal dot density for several different dot sizes. Each curve represents the Rayleigh scattering loss for a given quantum dot radius. The curves all terminate at the line that represents the maximum areal dot density for a given radius. For a particle of radius a , the maximum areal density, ρ_A , is $(4a^2)^{-1}$. As the radius of the quantum dot increases, the scattering loss also increases because of the strong dependence of C_{scat} on particle radius.

Atomic force microscopy images show that the areal density of quantum dots is $4\text{--}5 \times 10^{10} \text{ cm}^{-2}$, and the maximum dot radius is $14.7 \pm 2.5 \text{ nm}$. We choose the largest quantum dot dimension as the quantum dot radius because of the 6th power dependence of the scattering cross section, thus giving a worst case value for the scattering loss. From Fig. 4, these dimensions correspond to a scattering loss of $1.5\text{--}2.5 \text{ cm}^{-1}$. This is not enough to account for the high internal loss measured on the quantum dot laser. Current quantum dot lasers usually have a dot density of between 10^{10} and 10^{11} cm^{-2} . At these densities, the loss due to Rayleigh scattering is

of the same order as the other loss mechanisms in semiconductor lasers if the dot size is larger than about 24 nm (for a density of 10^{10} cm^{-2}) to 12 nm (for a density of 10^{11} cm^{-2}). If the dots are smaller than these values, then the Rayleigh scattering loss is insignificant compared to the other internal loss mechanisms. If quantum dots with a radius of less than about 8 nm are used, then Rayleigh scattering will not be an important loss mechanism for quantum dot lasers with infrared wavelengths.

The above model for Rayleigh scattering assumes single-particle scattering, which implies that the dot density is such that there is only one or fewer dots per wavelength of light. The dots in the laser described earlier clearly do not satisfy this criterion. If the particle density corresponds to more than one dot per wavelength of light, then the photon may see a lower refractive index difference and thus be scattered less. Therefore, the curves shown in Fig. 4 can be regarded as the worst case scenario for Rayleigh scattering.

Although Rayleigh scattering is not important for the quantum dot lasers described in this paper, it might be an important scattering mechanism in other materials systems. For example, if instead of an infrared laser (emission $\approx 1000 \text{ nm}$) the calculations were repeated with a blue or ultraviolet laser that has a quantum dot active layer [18] the loss would increase by about two orders of magnitude due to the strong wavelength dependence of the scattering cross section (see Eq. (1)). A larger refractive index ratio between scatterer and surrounding medium would also increase the loss due to Rayleigh scattering. More accurate calculations would require using the exact shape of the quantum dot, including the imaginary component of the refractive index, and including multiple scatterers within one optical wavelength.

4. Conclusions

Quantum dot lasers using only a single layer of quantum dots have been measured from 80–300 K. The characteristic temperature of these lasers is slightly improved as compared to a similar quantum well laser. The quantum dot laser lases from excited states over the entire temperature range,

and this limits the characteristic temperature. The high internal loss in these quantum dot lasers cannot be explained by Rayleigh scattering, but it is possible that Rayleigh scattering may limit the performance of quantum dot lasers, especially blue and ultraviolet quantum dot lasers.

Acknowledgements

The authors thank Tom Reynolds, Dan Cohen, and Dan Tauber for the assistance with the measurements and helpful discussions. This work was supported by the NSF's Science and Technology Center for Quantized Electronic Structures (QUEST), Grant No. DMR 91-20007.

This paper is a contribution of the United States government by the National Institute of Standards and Technology (NIST) and is not subject to copyright.

References

- [1] Y. Arakawa, H. Sakaki, *Appl. Phys. Lett.* 40 (11) (1982) 939.
- [2] M. Asada, Y. Miyamoto, Y. Suematsu, *IEEE J. Quantum Electron.* 22 (9) (1986) 1915.
- [3] L. Goldstein, F. Glas, J. Marzin, M. Charasse, G. LeRoux, *Appl. Phys. Lett.* 47 (10) (1985) 1099.
- [4] M. Tabuchi, S. Noda, A. Sasaki, in: S. Namba, C. Hamaguchi, T. Ando (Eds.), *Science and Technology of Mesoscopic Structures*, Springer, Tokyo, 1992.
- [5] D. Leonard, M. Krishnamurthy, C.R. Reaves, S.P. DenBaars, P.M. Petroff, *Appl. Phys. Lett.* 63 (23) (1993) 3203.
- [6] J.M. Moison, F. Houzay, F. Barthe, L. Leprince, E. Andre, O. Vatel, *Appl. Phys. Lett.* 64 (2) (1994) 196.
- [7] Q. Xie, A. Madhukar, P. Chen, N.P. Kobayashi, *Phys. Rev. Lett.* 75 (13) (1995) 2542.
- [8] G.S. Solomon, J.A. Trezza, A.F. Marshall, J.S. Harris, *Phys. Rev. Lett.* 76 (6) (1996) 952.
- [9] N. Kirstaedter, N.N. Ledentsov, M. Grundmann, D. Bimberg, V.M. Ustinov, S.S. Ruvimov, M.V. Maximov, P.S. Kop'ev, Zh.I. Alferov, U. Richter, P. Werner, U. Gösele, J. Heydenreich, *Electron. Lett.* 30 (17) (1994) 1416.
- [10] K. Kamath, P. Bhattacharya, T. Sosnowski, T. Norris, J. Phillips, *Electron. Lett.* 32 (15) (1996) 1374.
- [11] R. Mirin, A. Gossard, J. Bowers, *Electron. Lett.* 32 (18) (1996) 1732.
- [12] D. Bimberg, N. Ledentsov, M. Grundmann, N. Kirstaedter, O. Schmidt, M. Mao, V. Ustinov, A. Egorov, A. Zhukov, P. Kopev, Zh. Alferov, S. Ruvimov, U. Gosele, J. Heydenreich, *Jpn. J. Appl. Phys.* 35 (1996) 1311.
- [13] H. Shoji, Y. Nakata, K. Mukai, Y. Sugiyama, M. Sugawara, N. Yokoyama, H. Ishikawa, *Electron. Lett.* 32 (21) (1996) 2023.
- [14] H. Saito, K. Nishi, I. Ogura, S. Sugou, Y. Sugimoto, *Appl. Phys. Lett.* 69 (21) (1996) 314.
- [15] R.P. Mirin, J.P. Ibbetson, J.E. Bowers, A.C. Gossard, *J. Crystal Growth* 175/176 (1997) 696.
- [16] M. Kerker, *The Scattering of Light and Other Electromagnetic Radiation*, Academic Press, New York, 1969, p. 666.
- [17] L.A. Coldren, S. Corzine, *Diode Lasers and Photonic Integrated Circuits*, in: K. Chang (Ed.), *Wiley Series in Microwave and Optical Engineering*, 1st ed., Wiley, New York, 1995, p. 593.
- [18] S. Nakamura, M. Senoh, S. Nagahama, N. Iwasa, T. Yamada, T. Matsushita, Y. Sugimoto, H. Kiyoku, *Appl. Phys. Lett.* 69 (10) (1996) 1477.